NASA Contractor Report 174939

NASA-CR-174939
19850021931

Study of Second Order Upwind Differencing in a Recirculating Flow

S.V. Vanka

Argonne National Laboratory
Argonne, Illinois

June 1985

Prepared for
Lewis Research Center
Under Interagency Agreement FY145583N0606

National Aeronautics and
Space Administration

TABLE OF CONTENTS

NOMENCLATURE

A	Finite difference coefficient
C	Convective flux
D	Diffusive flux
d	Cavity depth
F	Right hand side of the equation $L\phi = F$
I	Restriction/prolongation operator
p	Pressure
R	Residual in the solution
Re	Reynolds number ($u_W d/\nu$)
S	Source term
u	x-direction velocity
u_W	Top wall u velocity
v	y-direction velocity
x,y	Coordinate directions
ρ	Fluid density
ϵ	Error tolerance
η	Smoothing factor
ν	Fluid kinematic viscosity
ϕ	General transport variable

STUDY OF SECOND ORDER UPWIND DIFFERENCING IN A RECIRCULATING FLOW

by

S. P. Vanka

ABSTRACT

In this study, we have investigated the accuracy and stability of the second order upwind differencing scheme originally suggested by Price et al., and recently used by several others. The solution algorithm employed is based on a coupled solution of the nonlinear finite-difference equations by the multigrid technique. Calculations have been made of the driven cavity flow for several Reynolds numbers and finite-difference grids. We observe that in comparison with the hybrid differencing, the second order upwind differencing is somewhat more accurate but it is not monotonically accurate with mesh refinement. Also, the convergence of the solution algorithm deteriorates with the use of the second order upwind differencing.

1. INTRODUCTION

The calculation of practical fluid flows through the numerical solution of the governing partial differential equations relies heavily on the accuracy and stability of the finite difference (or finite element) scheme. In several earlier studies [1-22], existing schemes have been assessed and modifications have been suggested. However, the quest for an optimal discretization procedure still continues. The main difficulty arises from the (nonlinear) convective terms expressed by first order spatial derivatives of the flow variables. For low cell Reynolds numbers (less than two), the central difference operator is both stable and second-order accurate. However, in many practical calculations, the cell Reynolds numbers are much larger than this value. If central differencing is used

when cell Reynolds numbers are greater than two, spurious oscillations are known to result. The suggested cure [17] is to use a blend of central and upwind differences, giving the acronymed "hybrid differencing scheme." The hybrid differencing scheme has been used in several earlier studies but has been shown to contain significant numerical diffusion. Unless considerable mesh refinement is undertaken, the solution can be in appreciable error.

The second order upwind differencing (original idea traced to Price et al., [23]) has been suggested as an alternate to first order upwind differencing. In this scheme (for the convective term) the value at a local node is connected to two upstream values rather than just one value. This scheme can be formally shown to have second order accuracy. Atias et al., [8] have used this scheme to study the driven cavity flow and the problem of impinging jet on a normal flat plate in conjunction with the stream-function vorticity approach. Wilkes and Thompson [24] have used the second order upwind scheme in the calculation of laminar and turbulent flow in sudden expansions and contractions. Recently Shyy and Correa [1] have used the scheme for the laminar driven cavity problem and other more complicated situations. These three studies have concluded that the second order upwind scheme is more accurate than the first order upwind formulation and can therefore be a substitute for the hybrid scheme.

In two parallel developments, the Quadratic Upstream Differencing Scheme (QUICK) and the Skew Upwind Differencing Scheme (SUDS) have been suggested as alternates to the first order differencing. In QUICK [21], the concept is to evaluate the convective flux out of an interface of a finite difference cell by fitting a parabola between two upstream and one downstream nodes containing that interface. In SUDS [22], on the other hand, the concept is different. Here first order upwind differencing is used, but it is applied along the skewed streamline passing through the interface in question. Thus, upwinding is used in a vector sense, rather than along the resolved flow directions. Both QUICK and SUDS have been evaluated in a number of recent studies [1,5,9] and are shown to be more accurate than the first order upwind scheme. However, in using these schemes, difficulties of convergence and overshooting of the results from known exact solutions have been reported. Recently [5] modifications to

SUDS scheme in the form of bounding the solutions have been investigated with moderate success.

In this study, the second order upwind differencing is incorporated into a recently developed efficient solution algorithm for computation of general fluid flows. The new solution algorithm [25,26] is significantly different from many others such as the SIMPLE (or its variants) algorithm used in several earlier investigations, in the form of the TEACH computer program [27]. The present algorithm, BLIMM (for Block-Implicit Multigrid Method), is based on a coupled solution of the momentum and continuity equations by the powerful multigrid technique. Used in conjunction with the hybrid differencing scheme (HDS) it was observed to provide much faster convergence than SIMPLE, converging typically in ten to twenty iterations even with finite difference grids as large as 512x512 nodes in the square cavity problem. Consequently, the CPU times were observed to be much smaller than those of the TEACH computer program. In this study, the stability and accuracy of the higher order scheme are critically assessed by comparing its performance with the hybrid scheme. The calculations have been made for the flow in a two dimensional square cavity with a moving top wall.

The present paper is outlined as follows. First, the second order upwind differencing is detailed and contrasted with the hybrid finite differencing scheme. Three alternate formulations of second order upwind differencing are shown. In Section 3, the solution algorithm is briefly explained. Section 4 details the calculations made for the driven cavity problem and their results. The experiences are discussed in Section 5.

2. SECOND ORDER UPWIND DIFFERENCING

Consider the one-dimensional scalar transport equation

$$u\phi_x - \nu\phi_{xx} = 0 \ , \qquad (1)$$

with some given boundary conditions. The finite difference form of the diffusion term $\nu\phi_{xx}$ can be expressed without any difficulty by the central difference operator. Thus

$$(\nu\phi_{xx})_i = \frac{\nu}{\delta x^2}(\phi_{i+1} - 2\phi_i + \phi_{i-1}) , \tag{2}$$

where i is the index counter for the finite difference nodes in x direction. δx is the mesh size.

Similarly, the convective term $(u\phi_x)$ can be expressed by a central difference operator

$$(u\phi_x)_i = \frac{u_i}{2\delta x}(\phi_{i+1} - \phi_{i-1}) . \tag{3}$$

However, with this formulation when the cell Peclet number $(u_i \delta x/\nu)$ is greater than 2, the coefficient of ϕ_i becomes negative. Consequently, the upwind formulation

$$\begin{aligned}(u\phi_x)_i &= \frac{u_i}{\delta x}(\phi_i - \phi_{i-1}) , \quad u_i > 0 , \\ &= \frac{u_i}{\delta x}(\phi_{i+1} - \phi_i) , \quad u_i < 0 ,\end{aligned} \tag{4}$$

is frequently used. The above upwind formulation has only first order accuracy compared with the second order accuracy for central differencing.

The second order upwind formulation which has a higher order truncation error is as follows

$$\begin{aligned}(u\phi_x)_i &= \frac{u_i}{2\delta x}(3\phi_i - 4\phi_{i-1} + \phi_{i-2}) , \quad u_i > 0 \\ &= \frac{u_i}{2\delta x}(-3\phi_i + 4\phi_{i+1} - \phi_{i+2}) , \quad u_i < 0 .\end{aligned} \tag{5}$$

This scheme has formally $O(\delta x^2)$ truncation error. Wilkes and Thompson [24] have shown that the scheme has quadratic convergence to the exact solution, compared with linear convergence of the first order upwind scheme.

In order to implement the second order upwind scheme, a deferred correction procedure is frequently followed. That is, part of the differencing is written in terms of the coefficients linking the neighbor values and the remaining is treated explicitly as a source term. This enables a formulation that has a triagonal (in one dimension) or a pentadiagonal (two dimensions) matrix structure which is easy to solve. The deferred correction procedure is similar to the "curvature correction" used by Han et al., [13] in conjunction with the QUICK scheme.

The second order upwind differencing can be implemented in at least three ways, with varying degrees of implicitness and corresponding source terms. They are:

Scheme 1

$$(u\phi_x)_i = \frac{u_i}{\delta x}(\phi_i - \phi_{i-1}) + u_i \frac{(\phi_i - 2\phi_{i-1} + \phi_{i-2})}{2\delta x} + O(\delta x)^2 \text{ for } u_i > 0 ,$$

$$= \frac{u_i}{\delta x}(\phi_{i+1} - \phi_i) - \frac{u_i}{2\delta x}(\phi_{i+2} - 2\phi_{i+1} + \phi_i) + O(\delta x^2) \text{ for } u_i < 0 . \quad (6)$$

The first term is the upwind formulation; the second term is the explicit correction. The advantage with this formulation is that it can be easily implemented in a computer program that already uses the upwind differencing.

Scheme 2

Scheme 2 has been used by Wilkes and Thompson [24] and the terms are arranged as follows.

$$(u\phi_x)_i = \frac{3u_i}{2\delta x}(\phi_i - \phi_{i-1}) + \frac{u_i}{2\delta x}(\phi_{i-2} - \phi_{i-1}) + O(\delta x^2) \text{ for } u_i > 0 ,$$

$$= \frac{3u}{2\delta x}(\phi_{i+1} - \phi_i) - \frac{u_i}{2\delta x}(\phi_{i+2} - \phi_{i+1}) + O(\delta x^2) \text{ for } u_i < 0 . \quad (7)$$

In this formulation more implicitness is brought into the coefficient terms.

Scheme 3

Scheme 3 has been used by Atias et al., [8] and Shyy and Correa [1] with the following rearrangement.

$$(u\phi_x)_i = \frac{2u_i}{\delta x}(\phi_i - \phi_{i-1}) + \frac{u_i}{2\delta x}(\phi_{i-2} - \phi_i) + O(\delta x^2) \text{ for } u_i > 0 ,$$

$$= \frac{2u_i}{\delta x}(\phi_{i+1} - \phi_i) - \frac{u_i}{2\delta x}(\phi_{i+2} - \phi_i) + O(\delta x^2) \text{ for } u_i < 0 . \quad (8)$$

Scheme 3 has the largest coefficient term, having values twice those for Scheme 1. The three different formulations offer different degrees of implicitness in the solution of the equations. Thus their stability characteristics can be different. However, the final solution to the finite-difference equations is the same.

A. Boundary Conditions

Because the second order upwind differencing connects two upstream nodes, it is necessary to follow special practices for the finite difference nodes adjacent to a boundary; otherwise reference will have to be made to a value outside the flow domain. Atias et al., [8] have recommended switching back to first order upwind differencing for cells adjacent to a solid boundary. In Scheme 1 this implies setting the source term to zero for finite difference nodes i = 2 and i = (IMAX-1) (for a one dimensional problem). Shyy and Correa [1] have used the hybrid formulation near the boundaries. The hybrid formulation at boundaries is the same as the upwind formulation except that when the boundary cell Peclet number is less than two, central differencing is used. In the present work, the upwind differencing scheme, as used by Atias et al., is employed for the near-boundary cells.

B. Present Implementation

In this study, the second order upwind differencing is evaluated by calculating the laminar flow field in a square cavity with a moving top wall. The equations governing the flow are the two-dimensional momentum and

mass continuity equation for a planar flow, expressed as follows.

$$(uu)_x + (vu)_y = -\frac{\partial p}{\rho \partial x} + \nu(u_{xx} + u_{yy}) \ , \tag{9}$$

$$(vu)_x + (vv)_y = -\frac{\partial p}{\rho \partial y} + \nu(v_{xx} + v_{yy}) \ , \tag{10}$$

$$u_x + v_y = 0 \ . \tag{11}$$

A staggered mesh system has been used for storing the velocities and the pressures. The finite-difference equations are derived by integrating them over control volumes surrounding the velocities and the pressure. Because of the staggered mesh arrangement, these control volumes are different for the three equations, as shown in Figure 1.

In the present study, we have considered only Schemes 1 and 3. The performance of Scheme 2 is expected to be in between that of Scheme 1 and Scheme 3. In Scheme 1, the coefficients are assembled exactly as those for upwind differencing. The source term is calculated from existing values in store and is added to the right hand side. The general form of the finite difference equation is

$$A_C \phi_{i,j} = A_N \phi_{i,j+1} + A_S \phi_{i,j-1} + A_E \phi_{i+1,J} + A_W \phi_{i-1,j} + S(\phi)_{i,j} + P_{i,j} \ , \tag{12}$$

where $\phi_{i,j}$ represents $u_{i,j}$ and $v_{i,j}$. For a uniform mesh of δx and δy intervals in x and y directions, A_C, A_N, A_S, etc. are given by

$$A_C = A_N + A_S + A_E + A_W \ , \tag{13}$$

$$A_W = \max(0, C_{x-}) + D_{x-} \ , \tag{14}$$

$$A_E = \max(0, -C_{x+}) + D_{x+} \ , \tag{15}$$

$$A_S = \max(0, C_{y-}) + D_{y-} \ , \tag{16}$$

$$A_N = \max(0, -C_{y+}) + D_{y+} \ , \tag{17}$$

where

$$C_{x-} = (u)_{x-}\delta y \ , \ C_{x+} = u_{x+}\delta y \ , \tag{18}$$

$$C_{y-} = v_{y-}\delta x \ , \ C_{y+} = v_{y+}\delta x \ , \tag{19}$$

$$D_{x-} = \nu\delta y/\delta x \ , \ D_{x+} = \nu\delta y/\delta x \ , \tag{20}$$

$$D_{y-} = \nu\delta x/\delta y \ , \ D_{y+} = \nu\delta x/\delta y^{*} \ . \tag{21}$$

The term $S(\phi)_{i,j}$ is the correction term and is implemented as

$$\begin{aligned} S(\phi)_{i,j} = \frac{1}{2} \big[& C_W(\phi_{i-2,j} - 2\phi_{i-1,j} + \phi_{i,j}) \\ & + C_E(\phi_{i+2,j} - 2\phi_{i+1,j} + \phi_{i,j}) \\ & + C_S(\phi_{i,j-2} - 2\phi_{i,j-1} + \phi_{i,j}) \\ & + C_N(\phi_{i,j+2} - 2\phi_{i,j+1} + \phi_{i,j}) \big] \ . \end{aligned} \tag{22}$$

where

$$C_W = \max\,(0,\ C_{x-}) \ , \ C_E = \max\,(0,\ -C_{x+}) \ , \text{ etc.}$$

The value of $S(\phi)$ is zero for the lines of cells i = 2, j = 2, i = IMAX-1 and j = JMAX-1. $P_{i,j}$ represents the finite-difference form of the pressure term.

Scheme 3 is implemented much like Scheme 1, but the values of the convective terms in A_W, A_E, etc. are doubled. Thus

$$\begin{aligned} A_W &= \max(0,\ \ 2C_{x-}) + D_{x-} \ , \\ A_E &= \max(0,\ -2C_{x+}) + D_{x+} \ , \text{ etc.} \end{aligned} \tag{23}$$

---

*For near-boundary cells the distances are half the cell dimensions for the velocity component parallel to the boundary.

The source term $S(\phi)_{i,j}$ is given by

$$S(\phi)_{i,j} = \frac{1}{2} [C_W (\phi_{i-2,j} - \phi_{i,j}) + C_E (\phi_{i+2,j} - \phi_{i,j}) + C_S (\phi_{i,j-2} - \phi_{i,j}) + C_N (\phi_{i,j+2} - \phi_{i,j})] \quad (24)$$

Again, for the near-boundary cells, $S(\phi)_{i,j}$ is set to zero and coefficients A_W, A_E, etc., are reevaluated as in Equations (14) - (17).

In contrast with the second order upwind differencing, the hybrid formulation uses a combination of first order upwind differencing and second order central differencing. In the hybrid formulation, central differencing is used on both convection and diffusion terms, but when the cell Reynolds number is greater than two, upwinding is used on the convection term and the diffusion is set to zero. The corresponding expressions for the coefficients are:

$$A_W = \max (|C_{x-}| , D_{x-}) + C_{x-} \quad (25)$$

$$A_E = \max (|C_{x+}| , D_{x+}) - C_{x+} \quad (26)$$

$$A_S = \max (|C_{y-}| , D_{y-}) + C_{y-} \quad (27)$$

$$A_N = \max (|C_{y+}| , D_{y+}) - C_{y+} \quad (28)$$

3. SOLUTION ALGORITHM

In this study, the nonlinear finite-difference equations resulting from the second order upwind formulation are solved by a coupled multigrid algorithm. This algorithm was earlier used by the author in calculating the cavity flow, in conjunction with the hybrid differencing [25,26]. The

algorithm was observed to be rapidly convergent for large finite-difference grids (up to 514x514 grid nodes) and for very high Reynolds numbers (up to 5000).

The algorithm used here has two novel features. First, the momentum and continuity equations are solved simultaneously. Thus no pressure or pressure-correction equation is derived as is done in many earlier algorithms. Instead, the continuity equation is used in its primitive finite-difference form. Second, the coupled equations are solved iteratively by the multigrid technique [28]. The complete details of the present algorithm are given in references [25] and [26]. They are described here briefly.

A. Solution Cycle

In the present algorithm, the FAS-FMG (Full Approximation Storage - Full Multigrid) algorithm well suited for nonlinear problems is used. The FAS-FMG algorithm, flow charted in Figure 2, proceeds as follows. After a series of finite-difference grids is chosen, iterations are initiated on the coarsest grid (grid number 1). On this grid, the solution of the complete nonlinear problem is sought. The coefficients and the source terms in the finite-difference equations are evaluated with the existing values of velocities in store and the linear equations are then solved iteratively. The "relaxation procedure" used here is a Symmetrical Coupled Gauss-Siedel technique (SCGS). The SCGS was observed to provide good smoothing (i.e., convergence) rates for the hybrid scheme and is also used in this study. Basically, the SCGS scheme is a node by node solver; however, at each node, it updates all four velocities (i.e., on the four faces of the two-dimensional cell) and the pressure. The SCGS scheme solves five equations representing the complete transport characteristics at the node. In order to solve them, the equations are first written in terms of residuals and corrections at node (i,j). A matrix of four diagonal elements and two bordered line elements is then constructed from the five equations. Because of the bordered structure, the matrix can be easily inverted to give analytical expressions for the corrections. Due to the nonlinearity of the convection terms, the corrections are underrelaxed before adding to the flow

variables. The SCGS scheme is repeatedly applied at all nodes, updating the coefficients A_N, A_S, etc., and the source terms within the iterative sweeps. Such sweeps are performed until the residuals have decreased below the prescribed tolerance level. The tolerance is applied to the summed averaged residual (suitably normalized) over the whole flow domain.

After a converged solution on grid 1 is obtained, it is prolongated (extrapolated) to the next finest grid (grid 2). The solution on grid 2 is then sought. The coefficients are dynamically calculated inside the loop and at each node the five equations are solved. However, on this grid, the iterations are <u>not</u> carried until complete convergence. Instead, the rate of decrease of the averaged residual is monitored and when this rate falls below a specified rate, i.e., when

$$R_{p+1}/R_p > \eta \tag{29}$$

(where subscript p here refers to iteration count), the iterations on this grid are temporarily halted. The residuals and the solution are then restricted to the next coarser grid. The coefficients are formulated on the coarser grid with the restricted values of the flow variables, and a solution to the coarse grid equations is sought. The equations solved on the coarser grid (say grid 1) are

$$L^1 q^1 = F^1 + I_2^1 (F^2 - L^2 q^2) , \tag{30}$$

where I_2^1 restricts the residual $(F^2 - L^2 q^2)$ to grid 1. For the coarsest grid in the series of grids, Eq. (30) is solved exactly.

The solution on grid 1 is now used to correct the solution on grid 2. At this stage, the <u>solution</u> on grid 1 is not prolongated to grid 2, rather the <u>difference</u> between the initial and final solution on grid 1 is prolongated. Thus the correction to q^2 (the superscripts here correspond to grid numbers and are not exponents) is

$$q^2_{new} = q^2_{old} + I_1^2 \ (q^1 - I_2^1 \ q^2_{old}) . \tag{31}$$

The restrictions and prolongations between grids 1 and 2 are continued until an accurate solution on grid 2 is obtained. At this stage the solution on grid 2 is prolongated to grid 3 and the residuals are smoothed until the rate of smoothing falls below the threshold value (η). Restrictions are then made from grid 3 to grid 2 and the residuals are iterated on grid 2 until the smoothing is satisfactory. Otherwise the remaining residuals of grid 2 are transferred to grid 1 and annihilated completely (i.e., to $\leq 10^{-4}$ accuracy). As the solution sequence proceeds, finer and finer grids are considered and converged solutions are obtained on each grid. When a converged solution is obtained on the finest grid, M, the solution is terminated.

The tolerance level on all grids except the coarsest is set to 10^{-3}. For the square cavity calculation, this represented a decrease of three orders of magnitude in the averaged residual. The tolerance on grid 1 is set to a smaller value (10^{-4}) in order to obtain a nearly exact coarse grid solution (or correction). However, the accuracy level on intermediate grids during restriction from a finer grid is reset to a lower value. When an intermediate grid is reached by restricting the residuals from a finer grid, the solution on the intermediate grid is not obtained to 10^{-3} level of accuracy. Instead the tolerance is reset to

$$\varepsilon_h = \Delta\, e_{h+1} \,, \tag{32}$$

where $\Delta = 0.2$ and e_{h+1} represents the value of the residual for grid (h+1).

B. Restriction and Prolongation Operators

The restriction and prolongation procedures are somewhat dictated by the staggered mesh arrangement. Restriction is used for transferring fine grid values to a coarse grid, whereas prolongation is used for extrapolating a coarse grid correction to a fine grid. The two operators are denoted by I_h^{h-1} and I_{h-1}^{h}, respectively where h denotes one of the grids. A frequent restriction operator is injection, i.e., the coarse grid value is taken to be the local fine grid value. Thus

$$q^{c}_{i,j} = q^{f}_{2i-1,2j-1} \quad , \tag{33}$$

where the superscripts c,f denote coarse and fine grid values. The injection operator is not applicable for the staggered mesh because of the different locations of variables on coarse and fine meshes (see Fig. 1). In the current study, the restrictions are made by averaging neighbor values. Let (ic,jc) and (if,jf) denote coarse and fine mesh indices, respectively. Also, let $u_{i+1/2,j}$ be referred to as u(i,j) and $u_{i-1/2,j}$ be referred to as u(i-1,j), etc. Then

$$if = 2(ic) - 1 \quad , \text{ and } \quad jf = 2(jc) - 1 \quad ,$$

$$u^{c}(ic,jc) = 1/2[u^{f}(if,jf) + u^{f}(if,jf-1)] \quad , \tag{34}$$

$$v^{c}(ic,jc) = 1/2[v^{f}(if,jf) + v^{f}(if-1,jf)] \quad , \tag{35}$$

$$p^{c}(ic,jc) = 1/4[p^{f}(if,jf) + p^{f}(if,jf-1) \quad ,$$

$$+ p^{f}(if-1,jf) \quad + p^{f}(if-1,jf-1)] \quad . \tag{36}$$

The prolongation relations are derived by a bilinear prolongation. For each coarse grid node, four fine grid values are calculated. The relations are given in Vanka [25].

4. RESULTS

In what follows, we shall present the results of calculations for the driven cavity flow situation using the combination of the second order upwind differencing and the coupled multigrid solution technique. A series of calculations employing several Reynolds numbers and finite-difference meshes has been completed. The calculations have been made with both Schemes 1 and 3 described above. The rates of convergence (i.e. decrease of residuals in the finite difference equations) are somewhat different for both schemes, but the converged solutions are the same. Therefore the converged solutions of only one of the schemes will be presented. The Reynolds numbers considered are 100, 400, and 600. For the last value, the

rate of convergence was quite slow and therefore larger Reynolds numbers were not considered. Several grids containing up to 80x80 finite difference cells were employed for each Reynolds number when convergence was possible. In order to test the relative stability of the second order upwind differencing vis-a-vis the hybrid formulation calculations were made also with the hybrid differencing. All calculations were initiated from zero velocity and pressure fields.

A. Re = 100

Calculations for Reynolds numbers of 100 were made with grids containing 10x10, 20x20, 40x40, and 80x80 internal cells. Further finer meshes were not considered because the 80x80 mesh provides grid independent results even with hybrid formulation. Figures 3-5 provide the rates of convergence of the three schemes for this Reynolds number. The iteration number corresponds to the fine grid and the residuals are the average summed normalized residuals in the momentum and continuity equation, defined as

$$R = \left[\sum\{(R^u_{i,j})^2 + (R^v_{i,j})^2 + (R^c_{i,j})^2\}/(IMAX*JMAX*3)\right]^{1/2} . \qquad (37)$$

The optimal relaxation factor for these calculations was 0.8 for all schemes. It is seen that the hybrid scheme converges fastest, followed by Scheme 1 and then Scheme 3. The CPU times for these calculations are given in Table 1. The CPU times, in general, are not proportional to the number of fine grid iterations because of the different number of iterations on the coarse grids.

Table 1. CPU Times* (sec) for Re = 100

Grid	Scheme 1	Scheme 3	Hybrid
10x10	0.40	0.59	0.37
20x20	1.81	2.26	1.18
40x40	5.87	7.89	4.05
80x80	31.67	30.01	17.5

*IBM 3033, FORTHX, OPT(2) Compiler

The results of the converged fields are presented in Figures 6-8 for the different grids considered. For brevity, only the u-velocity profiles along the vertical centerline are presented. For comparison, the result of the 80x80 calculation is considered as the exact solution. From these figures, it is seen that for Re = 100, both the schemes give equally good accuracy with just 20x20 nodes. For the 10x10 grid, however, the second order upwind scheme is slightly more accurate.

B. Re = 400

The next Reynolds number considered is 400. Calculations for this Reynolds number were made with grids consisting of 10x10, 20x20, 40x40, and 80x80 nodes. Another calculation with 160x160 nodes with the hybrid scheme is considered to be the exact solution. Figures 9-12 show the rates of convergence for the three schemes for the Reynolds number of 400. The hybrid scheme converged the fastest, in 14 iterations. The relaxation factor for the hybrid scheme was 0.8. For the second order upwind scheme, however, a more restrictive relaxation factor was necessary. On the coarser grids (10x10 and 20x20) a value of 0.6 was optimal. For finer meshes, it was necessary to reduce this value to 0.4. The number of iterations for the second order scheme was much larger than the number with the hybrid scheme. Thus, it is seen that the second order scheme is less stable at higher Reynolds number, a property that makes the scheme less attractive unless the additional accuracy gained more than compensates for the larger CPU time.

Figures 13-16 show the centerline velocity with the hybrid and second order schemes for Re = 400, obtained with the various grids. The exact solution corresponds to the hybrid calculation with a 160x160 grid. This figure shows that both the second order upwind and the hybrid schemes give incorrect results even with 40x40 cells. However, with the hybrid scheme as the grid is refined further, the results get close to the exact solution.

For the second order scheme, however, the solution does not approach the true solution in a monotonic way. For example, in some regions, the error in the 20x20 solution is more than that in the 10x10 solution.

Nevertheless, as the grid is refined to 80x80 nodes, the error decreases, but the solution still does not match the exact solution obtained with the 160x160 grid and the hybrid differencing. This feature of second order upwind differencing is somewhat disturbing. The CPU times for the Re = 400 calculations are given in Table 2.

Table 2. CPU Times* for Re = 400

Grid	Scheme 1	Scheme 3	Hybrid
10x10	0.66	1.18	0.50
20x20	5.375	5.131	1.93
40x40	25.01	33.00	7.10
80x80	90.50	141.85	22.81

*IBM 3033, FORTHX, OPT(2) Compiler

C. Re = 600

Calculations for Reynolds numbers of 600 were also made with grids consisting of 10x10, 20x20, 40x40, and 80x80. cells. For the hybrid scheme, the relaxation factor was 0.8, as before. However, the second order scheme was observed to require much more damping. It was necessary to lower the underrelaxation factor (equal values are used on both u and v velocities) to 0.4 and 0.3 at finer grids. Figures 17-20 show the rates of convergence of the three schemes at this Reynolds number. Again, the hybrid is the fastest converging differencing scheme. Table 3 gives the required CPU times for these calculations. The results for Re = 600 are shown in Figures 21-24. Again the behavior is similar to that observed for Re = 400 but with slightly larger "overshoots" from the exact solution.

Table 3. CPU Times* for Re = 600

Grid	Scheme 1	Scheme 3	Hybrid
10x10	0.74	1.56	0.54
20x20	9.11	8.43	2.11
40x40	30.11	30.19	8.88
80x80	196.00	192.52	28.74

*IBM 3033, FORTHX, OPT(2) Compiler

D. Higher Reynolds numbers

Higher Reynolds numbers of 800 and 1000 were also considered, but it was observed that the above described trends, i.e., poor convergence and overshoots continue to be amplified with increase in Reynolds number. The hybrid scheme on the other hand was stable up to Re = 5000 with 160x160 grids [25]. Further calculations with second order upwind scheme were therefore discontinued.

5. DISCUSSION

Our experiences with the second order upwind difference scheme combined with the coupled multigrid algorithm have been somewhat discouraging. At low Reynolds numbers we observe that the rate of convergence with second order upwind differencing is only slightly worse than with the hybrid scheme and the results are marginally better. At higher Reynolds numbers, the rate of convergence with the second order upwind scheme is significantly worse than the hybrid scheme. In addition, not much seems to have been gained in terms of improved accuracy. It is surprising that even with 80x80 nodes, the second order scheme has some error. Thus no clear benefits of using the higher order upwind scheme are observable.

In contrast with our observations, Wilkes and Thompson [24] conclude that the second order upwind differencing is advantageous over the hybrid scheme (i.e., first order upwind scheme) even after discounting for the

additional time required for convergence. However, their studies were made in sudden expansion flows at low Reynolds numbers. Also in sudden expansion flows, the recirculation zone is smaller and of lower intensity than in the cavity situation. As a result, they observe improved performance of the second order upwind differencing over the first order (or hybrid) scheme.

The conclusions by Shy and Correa [1] in a cavity flow are somewhat puzzling to us. They employed only 20x20 (equally spaced) cells but were able to calculate up to Reynolds number of 10,000. They employed the TEACH computer program, based on the SIMPLE technique. Our calculation procedure (which is observed to be very stable and rapidly convergent with the hybrid scheme) was not stable beyond Re = 800 unless prohibitively small relaxation factors are used. Also, the nature of the velocity profile presented by them (for Re = 1000) is different from our results at Re = 600. At this stage, the only difference we have identified between the two finite differencing procedures is their use of the hybrid formula at near-boundary cells versus our use of first order upwind formula. This appears to be a trivial difference and we do not feel this to be the reason behind the different observations.

Although the present conclusions appear to discourage the use of second order upwind differencing, we believe that it may still be possible to use the scheme and take advantage of the second order accuracy if the precise cause of the "overshooting" is identified and remedied. We are of the opinion that some form of blending, with a first order scheme may be used in selected regions that have the potential for overshooting. A combination of first order and second order differencing may produce results superior to those of the individual schemes. We believe that further study in this direction will be fruitful.

REFERENCES

1. W. Shyy and S. M. Correa, "A Systematic Comparison of Several Numerical Schemes for Complex Flow Calculations," AIAA Paper No. 85-0440, 1985.

2. W. Shyy, "Study of Finite Difference Approximations to Steady-State Convection-Dominated Flow Problems," General Electric Report 83CRD189, July 1983.

3. R. A. Beier, J. de Ris, and H. R. Baum, "Accuracy of Finite Difference Methods in Recirculating Flows," Numerical Heat Transfer, 6, 283-302, 1983.

4. G. DeVahl Davis, and G. D. Mallinson, "An Evaluation of Upwind and Central Difference Approximations by a Study of Recirculation Flow," Computers and Fluids, 4, 29-43, 1976.

5. R. W. Claus, G. M. Neely, S. A. Syed, and A. D. Gosman, "Reducing Numerical Diffusion for Incompressible Flow Calculations," paper presented at the Western States Combustion Institute Meeting, 1984.

6. M. M. Gupta, "A Survey of Some Second-Order Difference Schemes for the Steady-State Convection-Diffusion Equation," Int. J. Numerical Methods in Fluids, 3, 319-331, 1983.

7. M. M. Gupta and R. P. Manohar, "A Critique of a Second Order Upwind Scheme for Viscous Flow Problems," AIAA Journal, 16, 759-761, 1978.

8. M. Atias, M. Wolfshtein, and M. Israeli, "Efficiency of Navier-Stokes Solver," AIAA Journal, 15, 263-255, 1977.

9. M. A. Leschziner, "Practical Evaluation of Three Finite-Difference Schemes for the Computation of Steady-State Recirculating Flows," Computer Methods in Applied Mechanics and Engineering, 23, 293-312, 1980.

10. M. A. Leschziner and W. Rodi, "Calculation of Annular and Twin Parallel Jets Using Various Discretization Schemes and Turbulence Model Variants," ASME J. Fluids Engineering, 103, 352-360, 1980.

11. B. P. Leonard, "A Survey of Finite Differences with Upwinding for Numerical Modeling of Incompressible Convective Diffusion Equation," in Recent Advances in Numerical Methods in Fluids, Vol. 2, C. Taylor, ed., Pineridge Press, 1981.

12. S. A. Syed, L. M. Chiappetta, and A. D. Gosman, "Error Reduction Program - Final Report," NASA-CR-174776, NASA Lewis Res. Center, May 1985.

13. T. Han, J. A. C. Humphrey and B. E. Launder, "A Comparison of Hybrid and Quadratic-Upstream Differencing in High Reynolds Number Elliptic Flows," Computer Methods in Applied Mechanics and Engineering, 29, 81-95, 1981.

14. J. J. McGuirk, A. M. K. P. Taylor and J. H. Whitelaw, "The Assessment of Numerical Diffusion in Upwind Difference Calculations of Turbulent Recirculating Flows," Third Symposium on Turbulent Shear Flows, L. J. S. Bradbury et al., (eds), Springer-Verlag, Berlin, 1982.

15. A. Pollard and A. L. W. Siu, "The Calculation of Some Laminar Flows Using Various Discretization Schemes," Computer Methods in Applied Mechanics and Engineering, 35, 293-313, 1982.

16. R. M. Smith and A. G. Hutton, "The Numerical Treatment of Advection: A Performance Comparison of Current Methods," Numerical Heat Transfer, 5, 439-461, 1982.

17. D. B. Spalding, "A Novel Finite-Difference Formulation for Differential Expressions Involving Both First and Second Derivatives," Int. J. Numerical Methods in Engineering, 4, 551-559, 1972.

18. S. P. Vanka, "Accuracy of the Finte Analytic Method for Scalar Transport Calculations," ANL-84-63, Argonne National Laboratory, Argonne, IL, 1984.

19. C. J. Chen, H. Naseri-Nashat, and K. S. Ho, "Finite Analytic Numerical Solution of Heat Transfer in Two-Dimensional Cavity Flow," J. of Numerical Heat Transfer, 4, 179-197, 1981.

20. G. D. Stubley, G. D. Raithby, and A. B. Strong, "A Proposal for a New Discrete Method Based on an Assessment of Discretization Errors," Numerical Heat Transfer, 3, 411-428, 1980.

21. B. P. Leonard, "A Stable and Accurate Convective Modeling Procedure Based on Quadratic Upstream Interpolation," Computer Methods Applied Mechanics and Engineering, 19, 59-98, 1979.

22. G. D. Raithby, "Skew Upstream Differencing for Problems Involving Fluid Flow," Computer Methods in Applied Mechanics and Engineering, 9, 153-164, 1976.

23. H. S. Price, R. S. Varga and J. E. Warren, "Applications of Oscillation Matrices to Diffusion-Correction Equations," Journal of Mathematics and Physics, 45, 301-311, 1966.

24. N. S. Wilkes and C. P. Thompson, "An Evaluation of Higher-order-upwind Differencing for Elliptic Flow Problems," Numerical Methods in Laminar and Turbulent Flows, Pineridge Press, UK, 248-257, 1983.

25. S. P. Vanka, "Block-Implicit Multigrid Solution of Navier-Stokes Equations in Primitive Variables," submitted for publication, 1985.

26. S. P. Vanka, "A Calculation Procedure for Three-dimensional Recirculating Flows," submitted for publication, 1985.

27. A. D. Gosman, F. J. K. Ideriah, "TEACH-T: A General Computer Program for Two-Dimensional Turbulent, Recirculating Flows," Department of Mechanical Engineering Report, Imperial College, 1976.

28. A. Brandt, "Guide to Multigrid Development," in Multigrid Methods, Lecture Notes in Mathematics, 960, Springer-Verlag, Berlin, 1982.

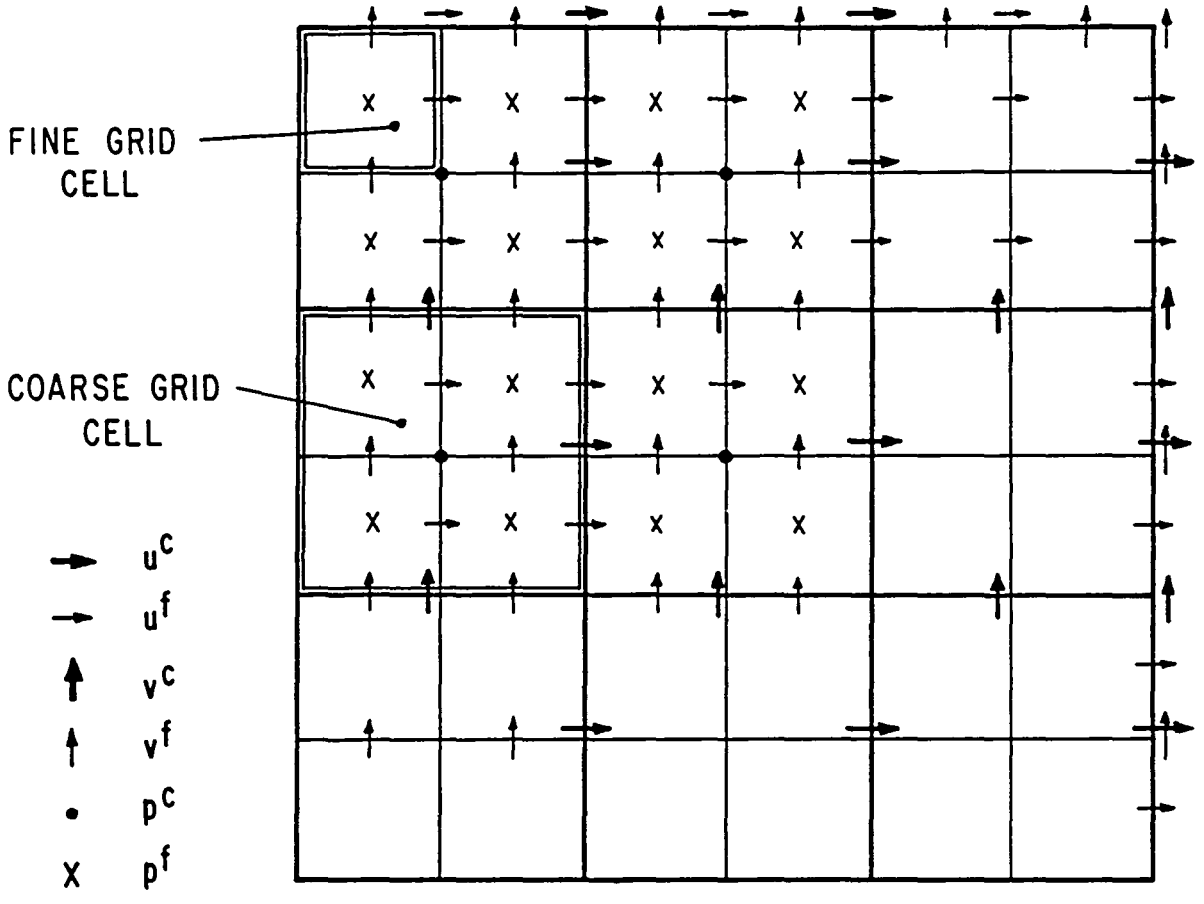

Fig. 1. Staggered Mesh Arrangement

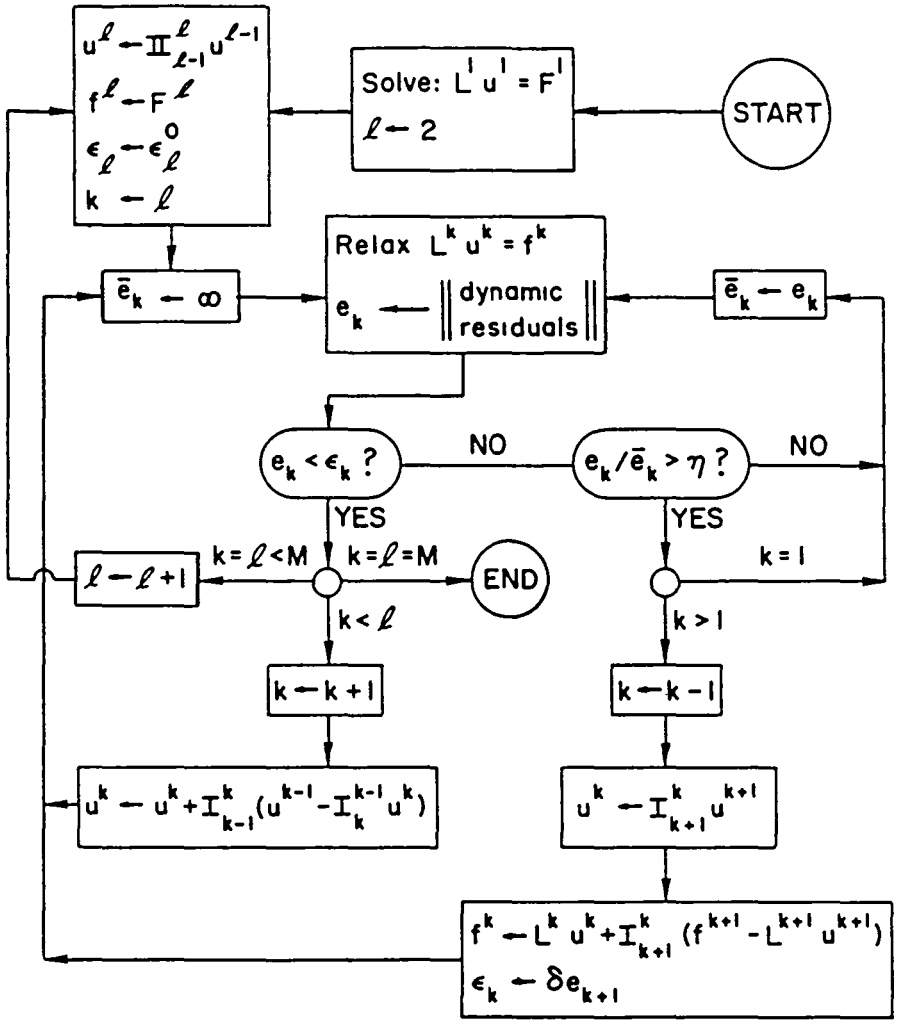

Fig. 2. Solution Cycle

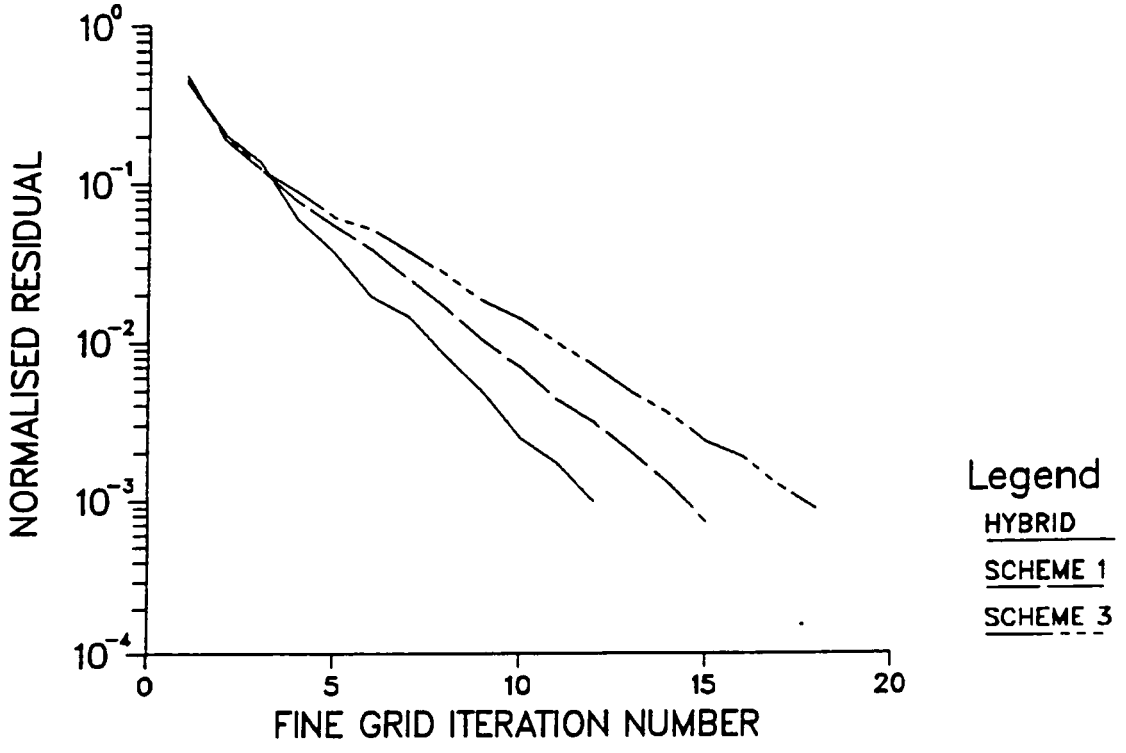

Fig. 3. Rates of Convergence, Re = 100, 10x10 Grid

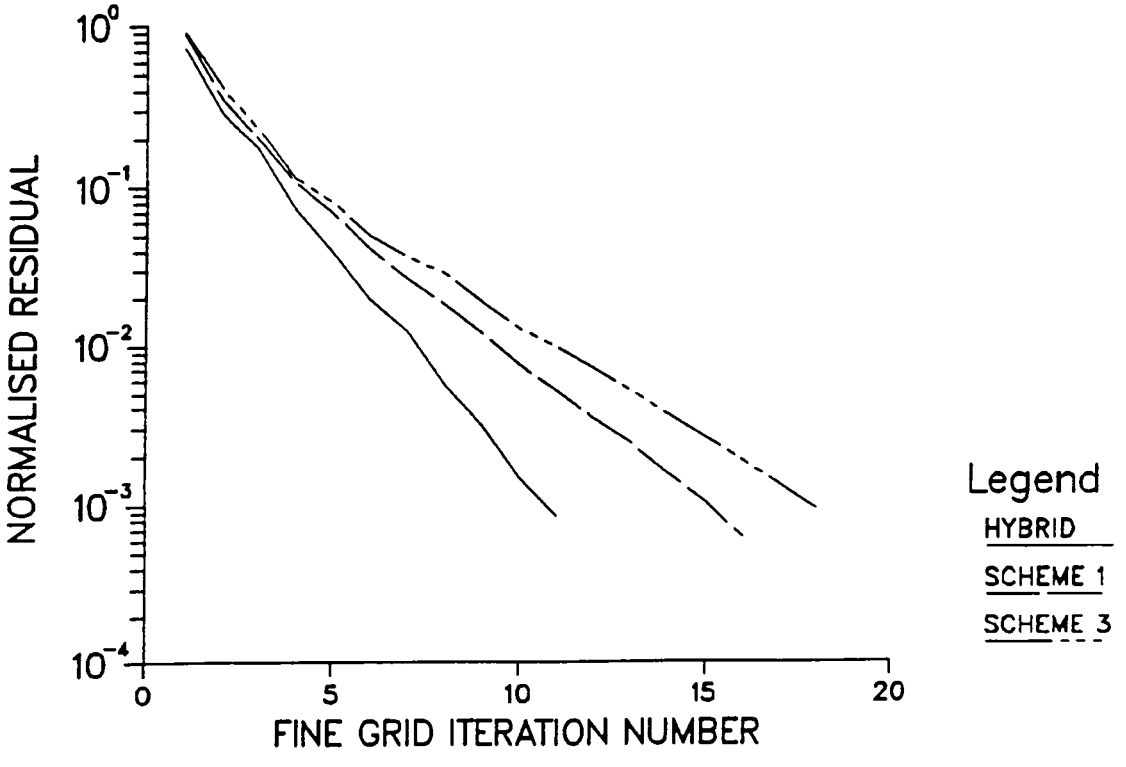

Fig. 4. Rates of Convergence, Re = 100, 20x20 Grid

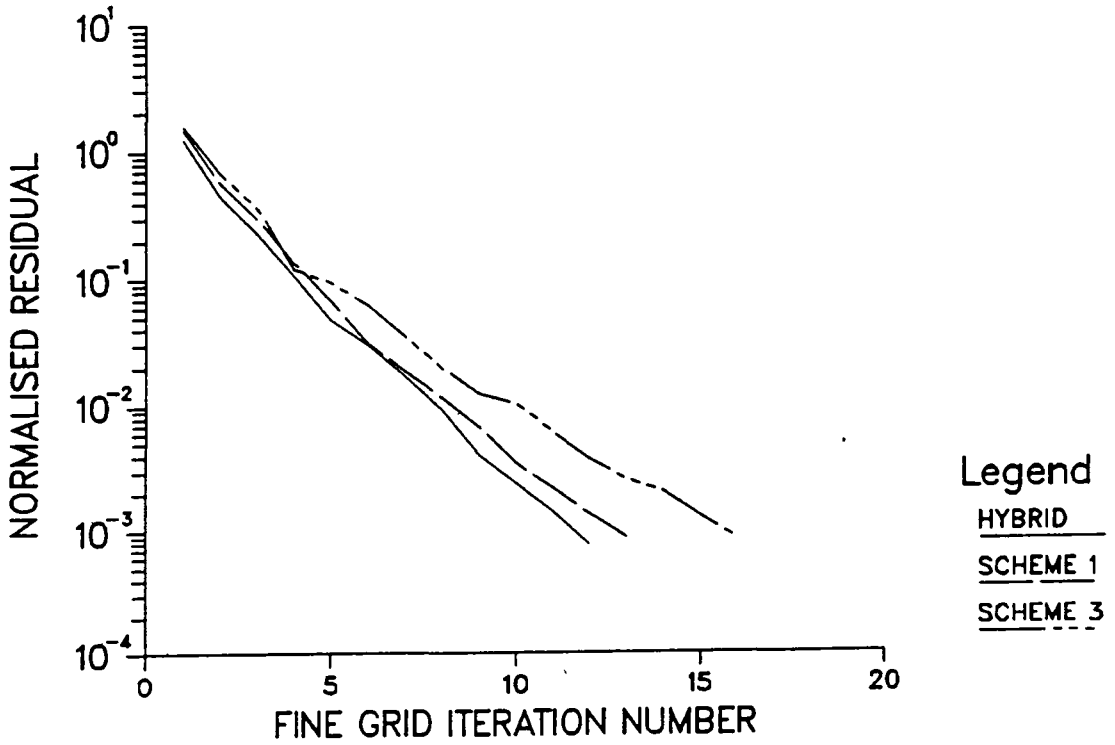

Fig. 5. Rates of Convergence, Re = 100, 40x40 Grid

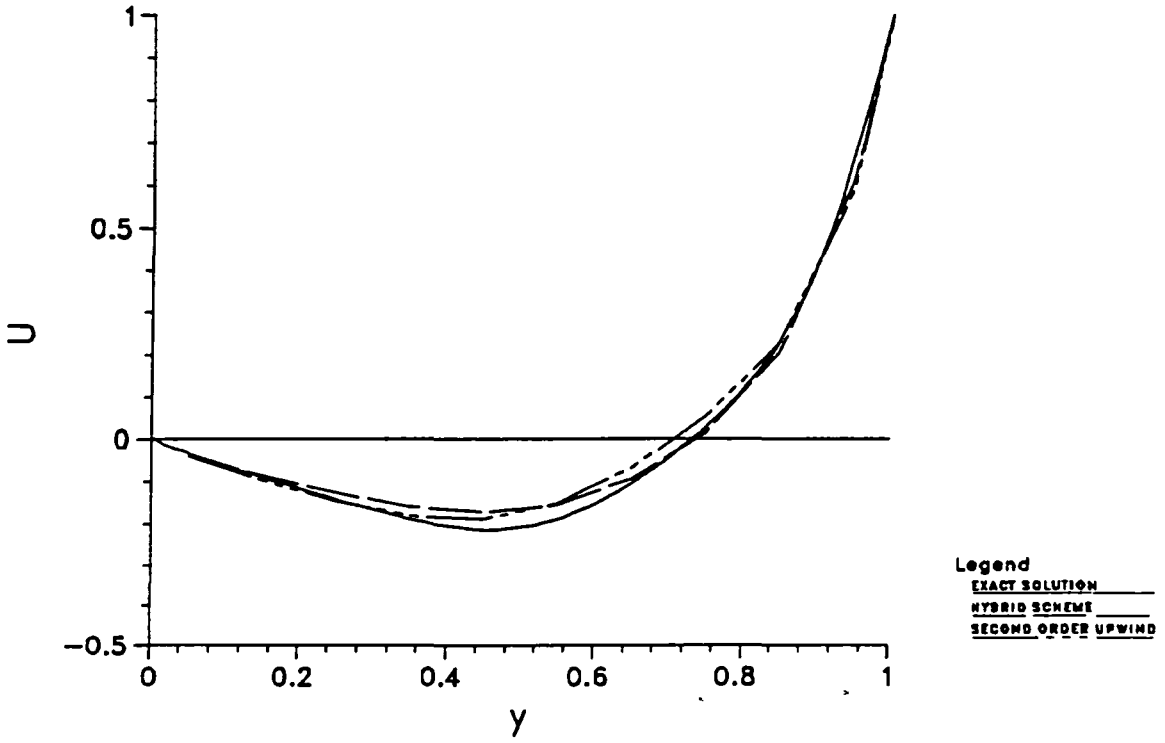

Fig. 6. Comparison of Vertical Center-line u-velocity Profile for Re = 100, 10x10 Grid

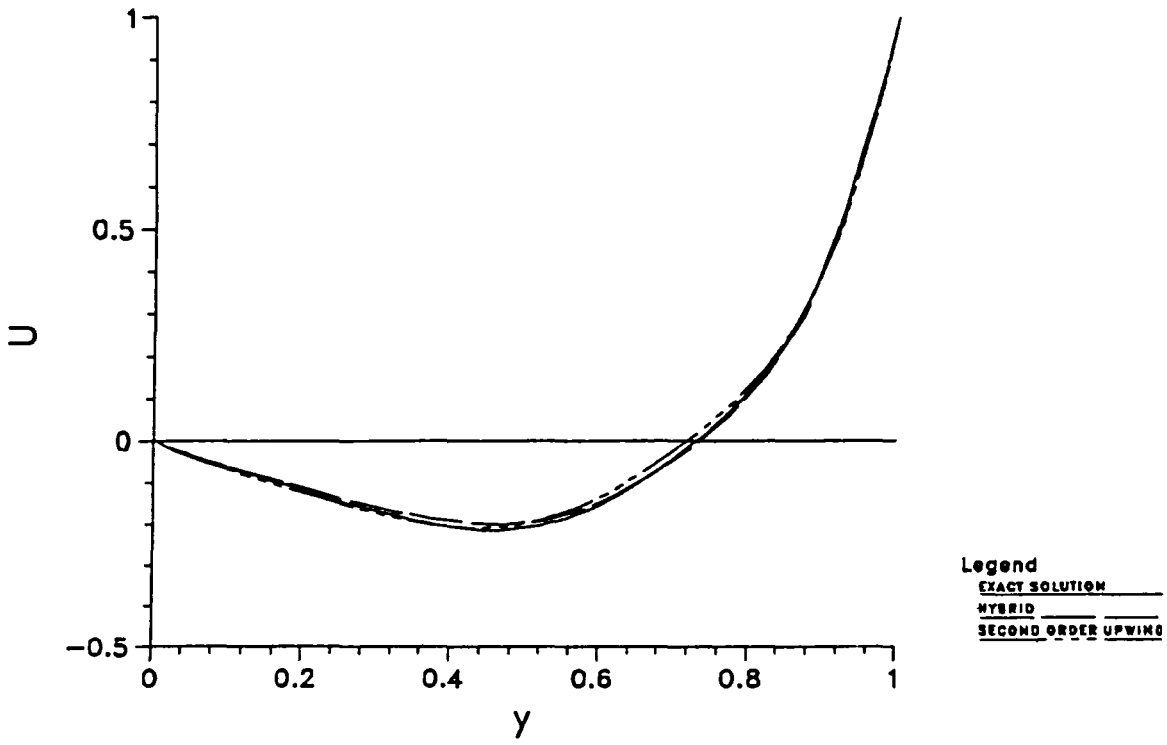

Fig. 7. Comparison of Vertical Center-line u-velocity Profile for Re = 100, 20x20 Grid

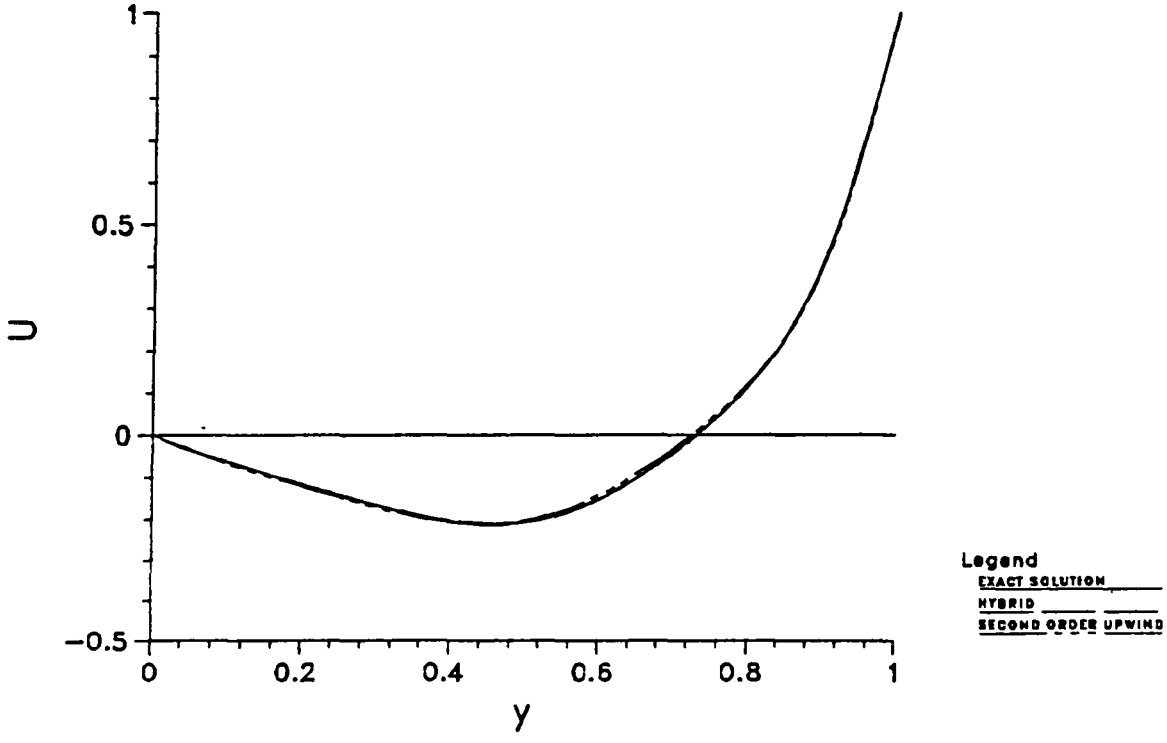

Fig. 8. Comparison of Vertical Center-line u-velocity Profile for Re = 100, 40x40 Grid

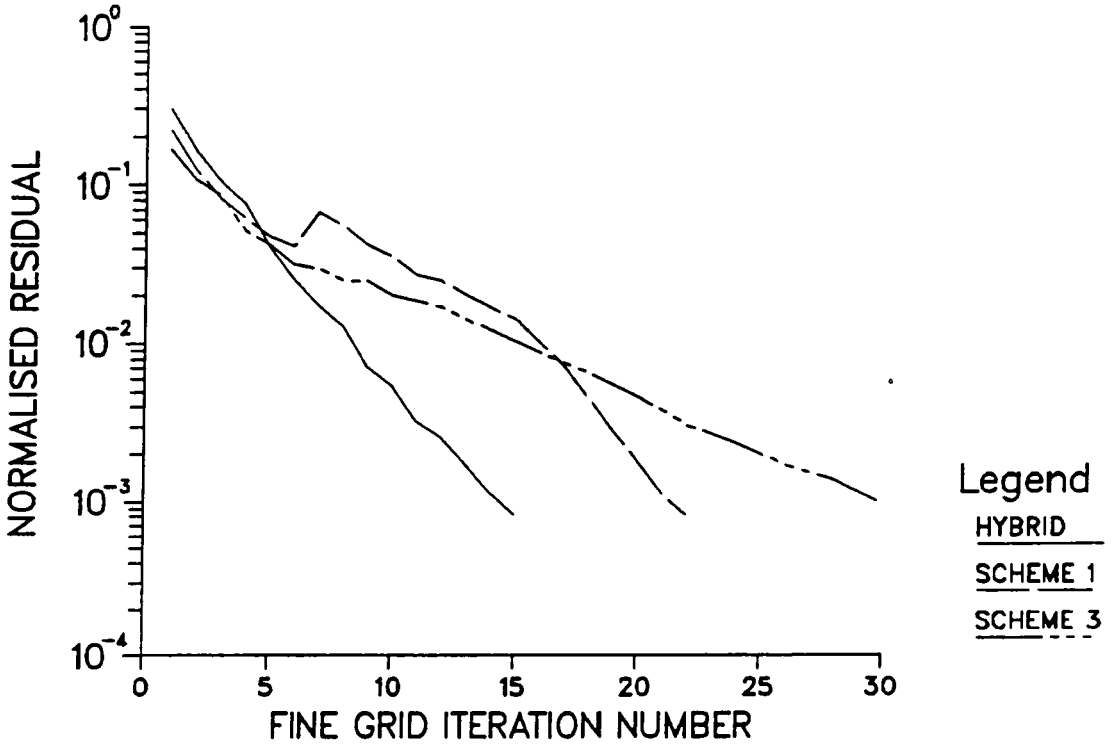

Fig. 9. Rates of Convergence, Re = 400, 10x10 Grid

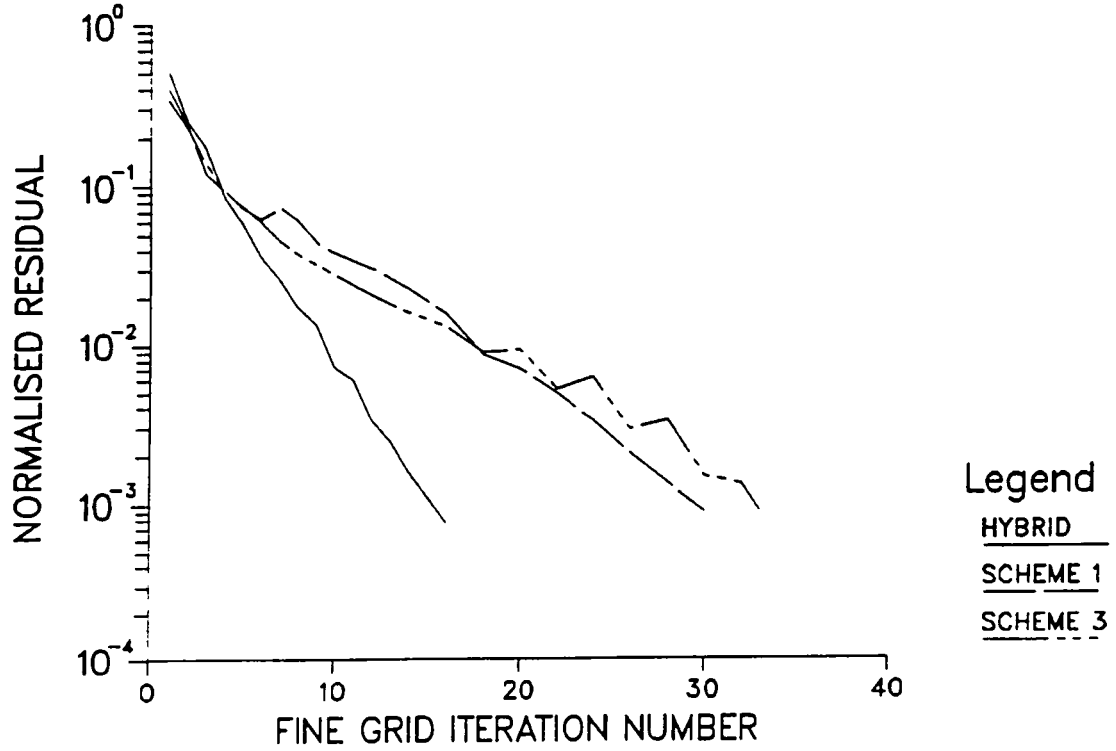

Fig. 10. Rates of Convergence, Re = 400, 20x20 Grid

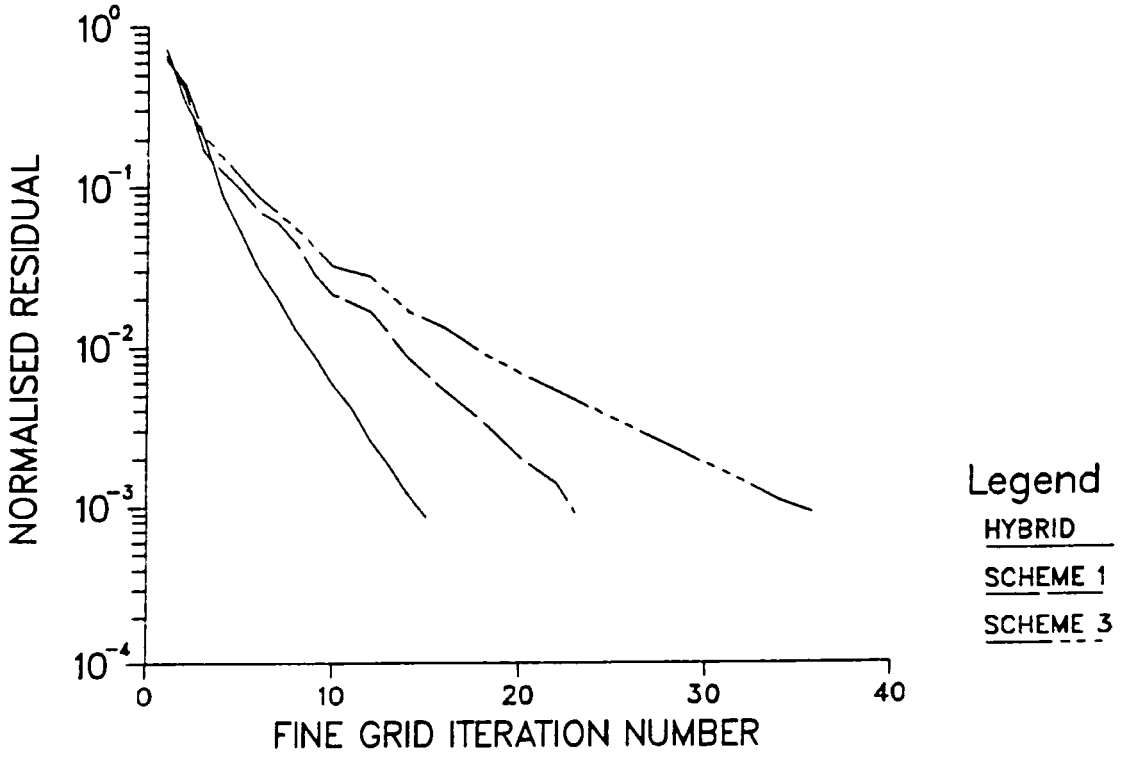

Fig. 11. Rates of Convergence, Re = 400, 40x40 Grid

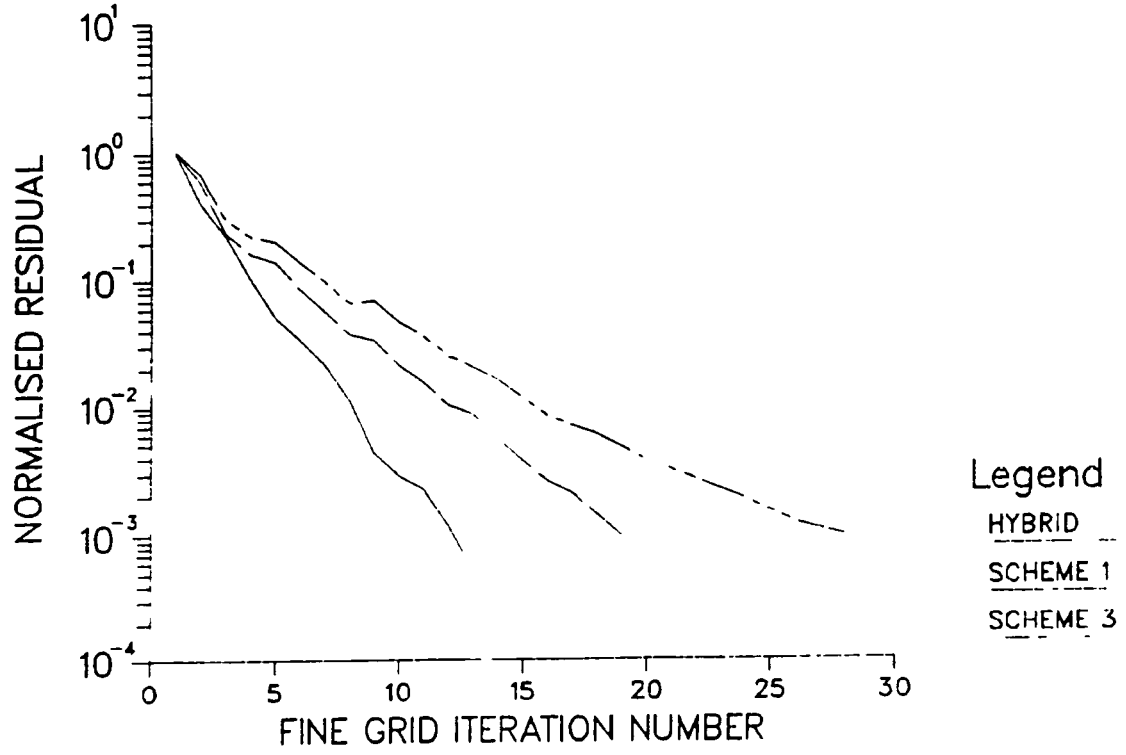

Fig. 12. Rates of Convergence, Re = 400, 80x80 Grid

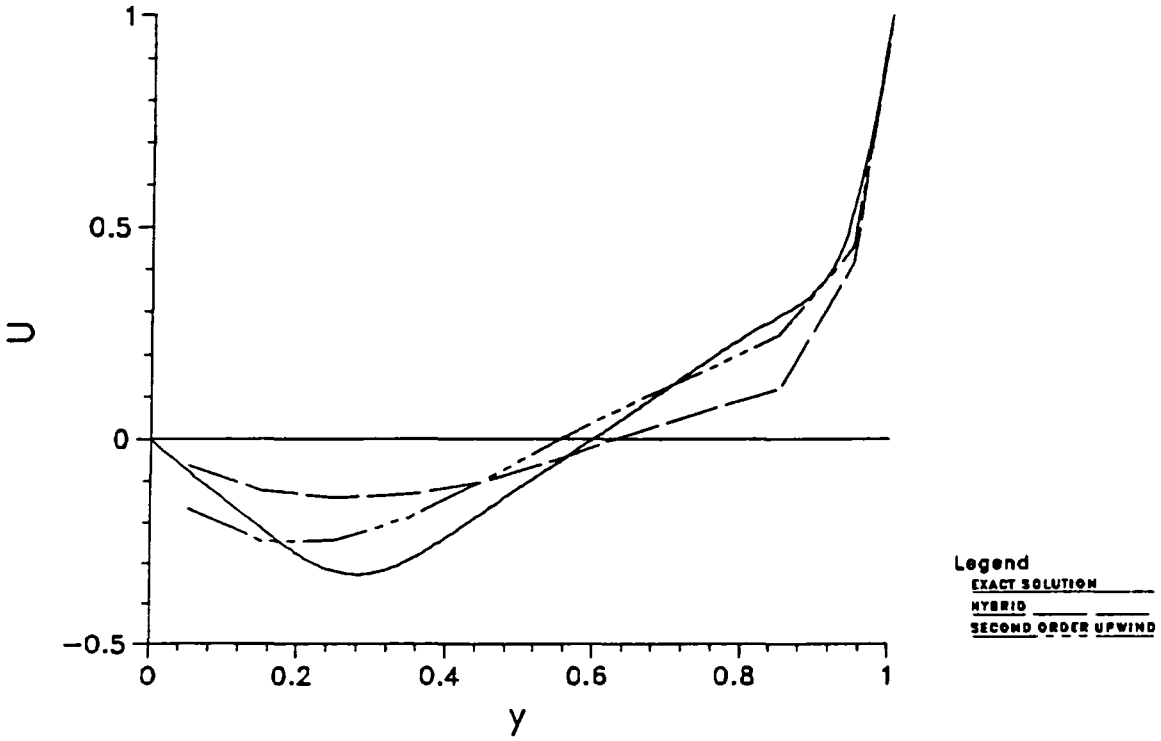

Fig. 13. Comparison of Vertical Center-line u-velocity Profile for Re = 400, 10x10 Grid

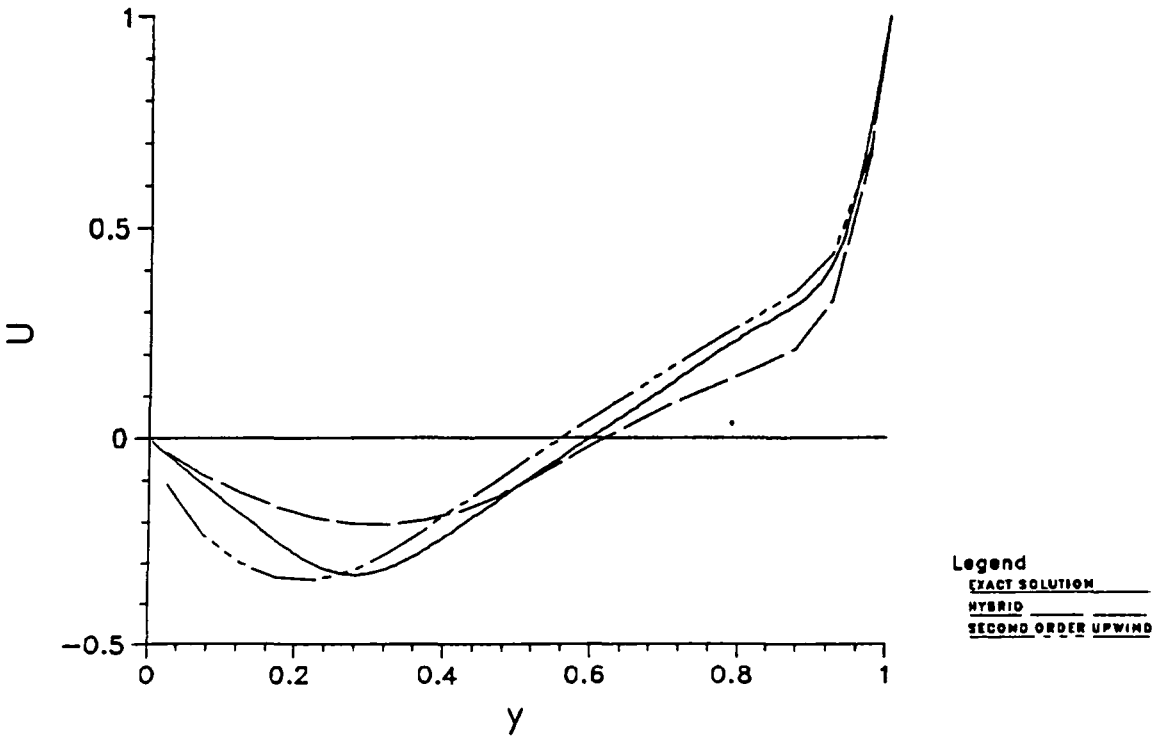

Fig. 14. Comparison of Vertical Center-line u-velocity Profile for Re = 400, 20x20 Grid

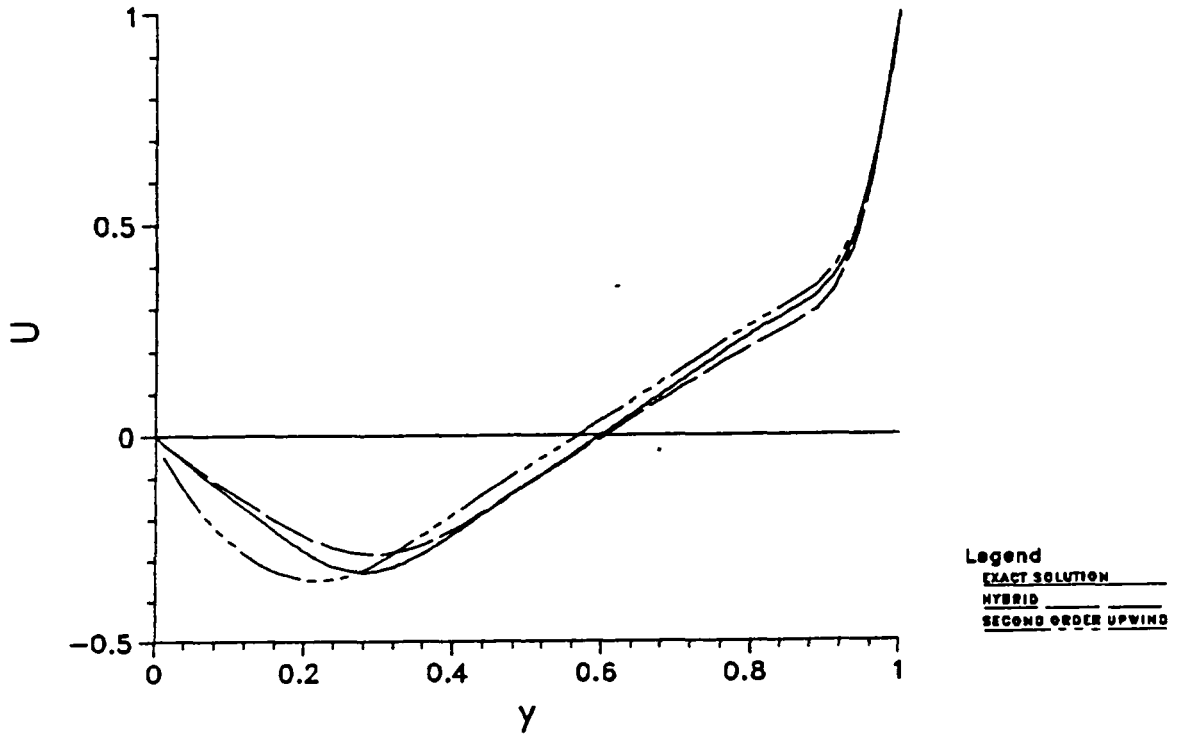

Fig. 15. Comparison of Vertical Center-line u-velocity Profile for Re = 400, 40x40 Grid

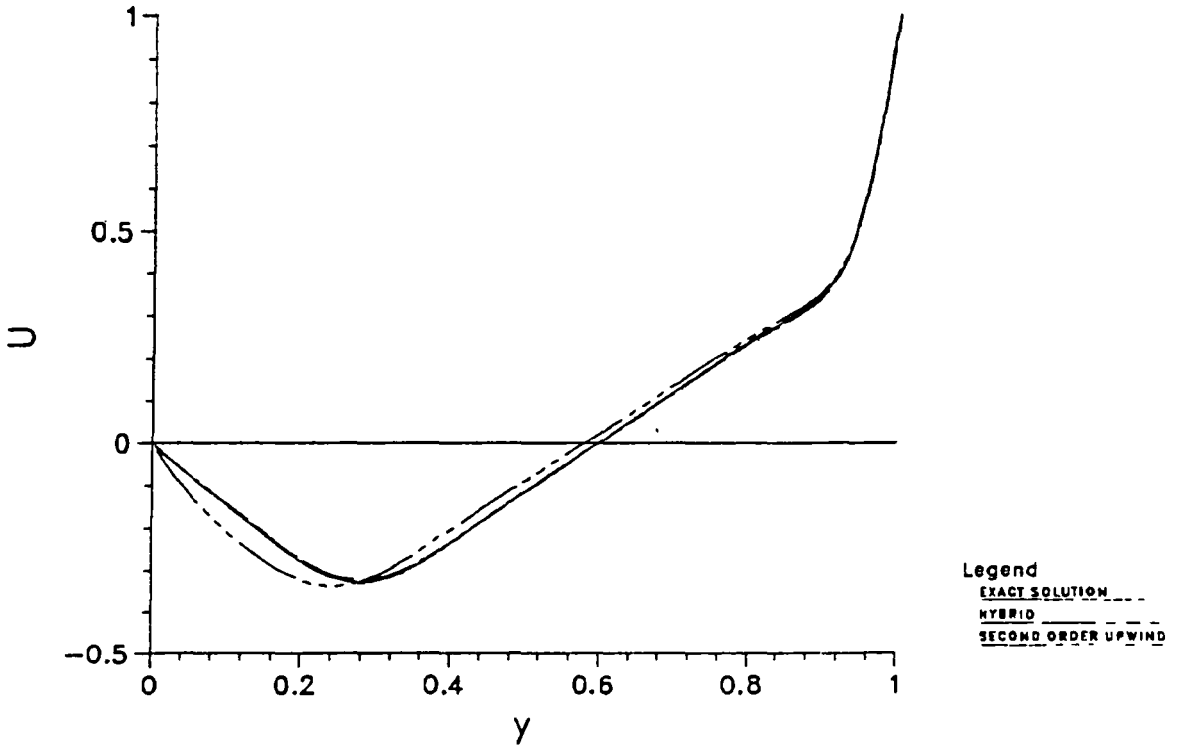

Fig. 16. Comparison of Vertical Center-line u-velocity Profile for Re = 400, 80x80 Grid

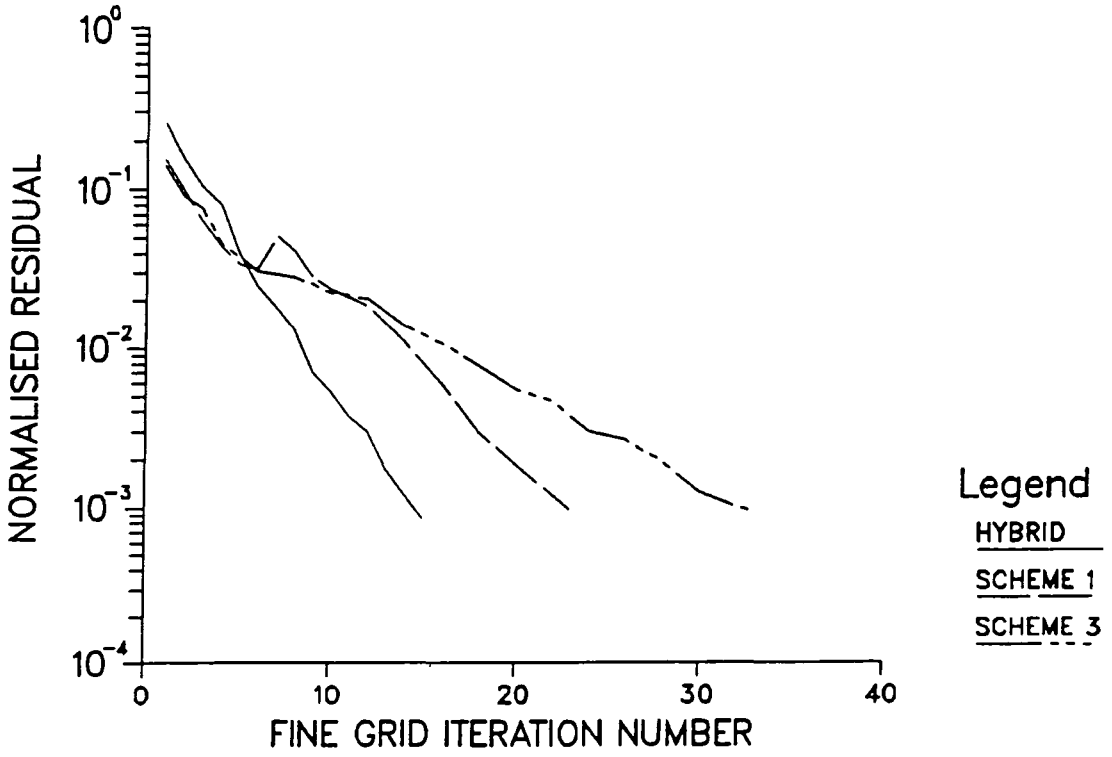

Fig. 17. Rates of Convergence, Re = 600, 10x10 Grid

Fig. 18. Rates of Convergence, Re = 600, 20x20 Grid

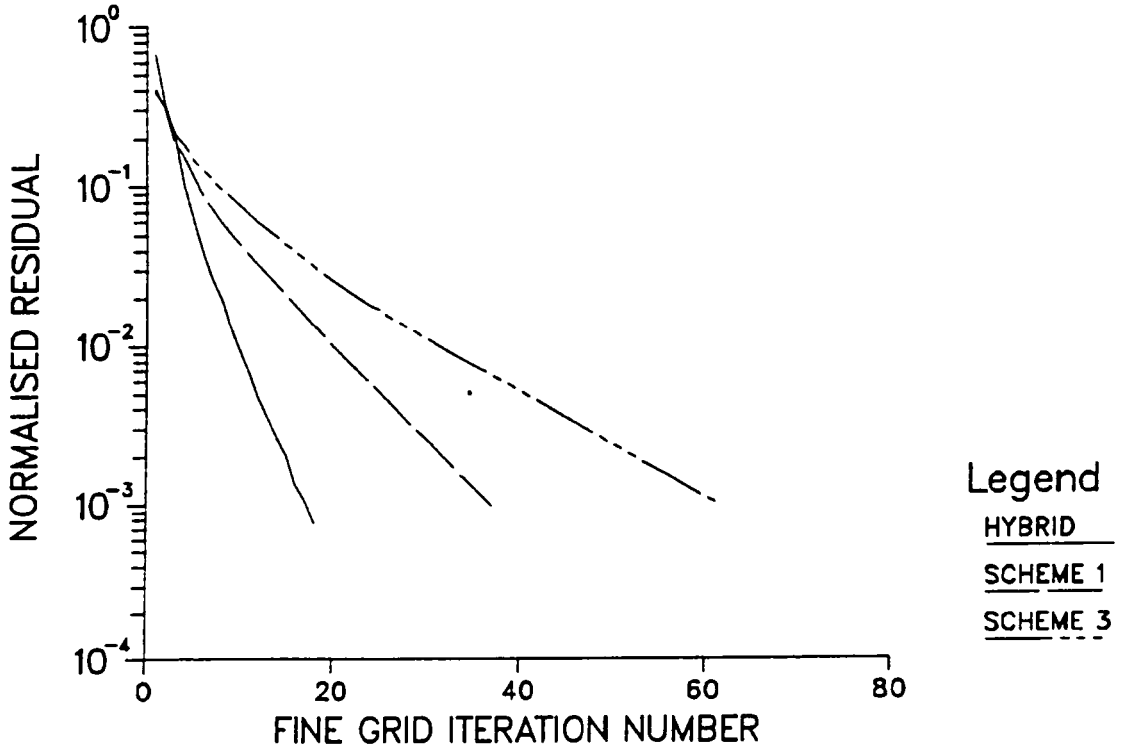

Fig. 19. Rates of Convergence, RE = 600, 40x40 Grid

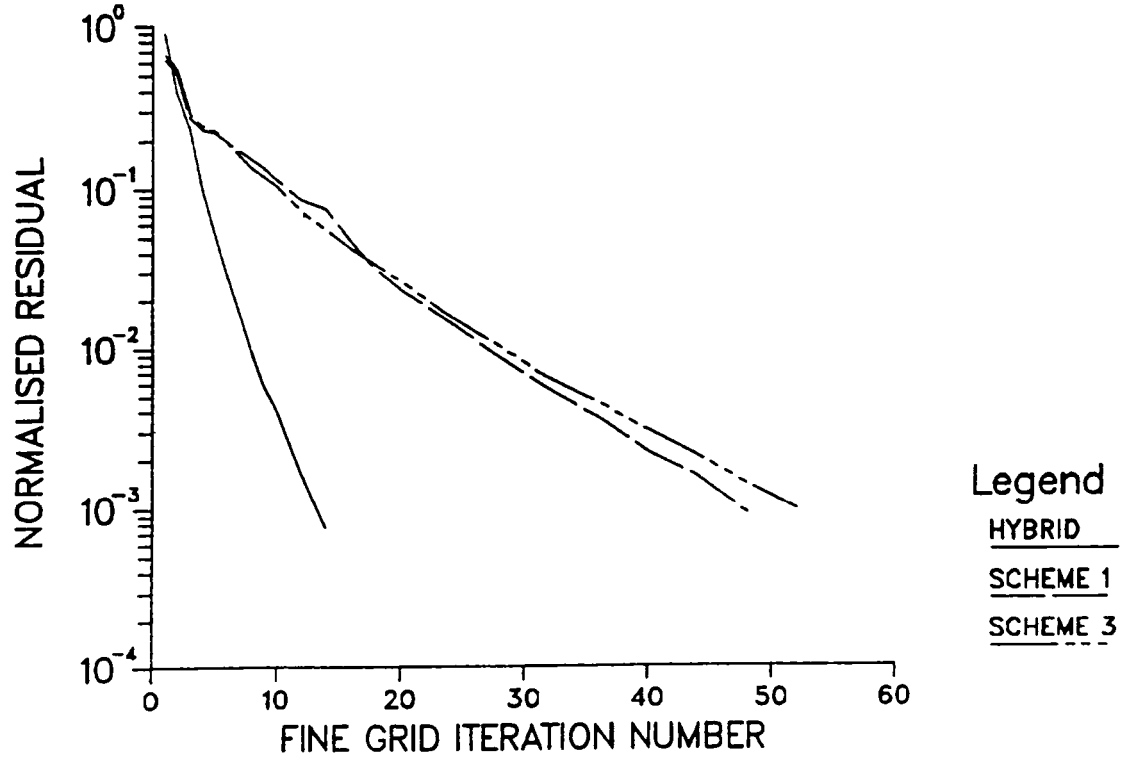

Fig. 20. Rates of Convergence, Re = 600, 80x80 Grid

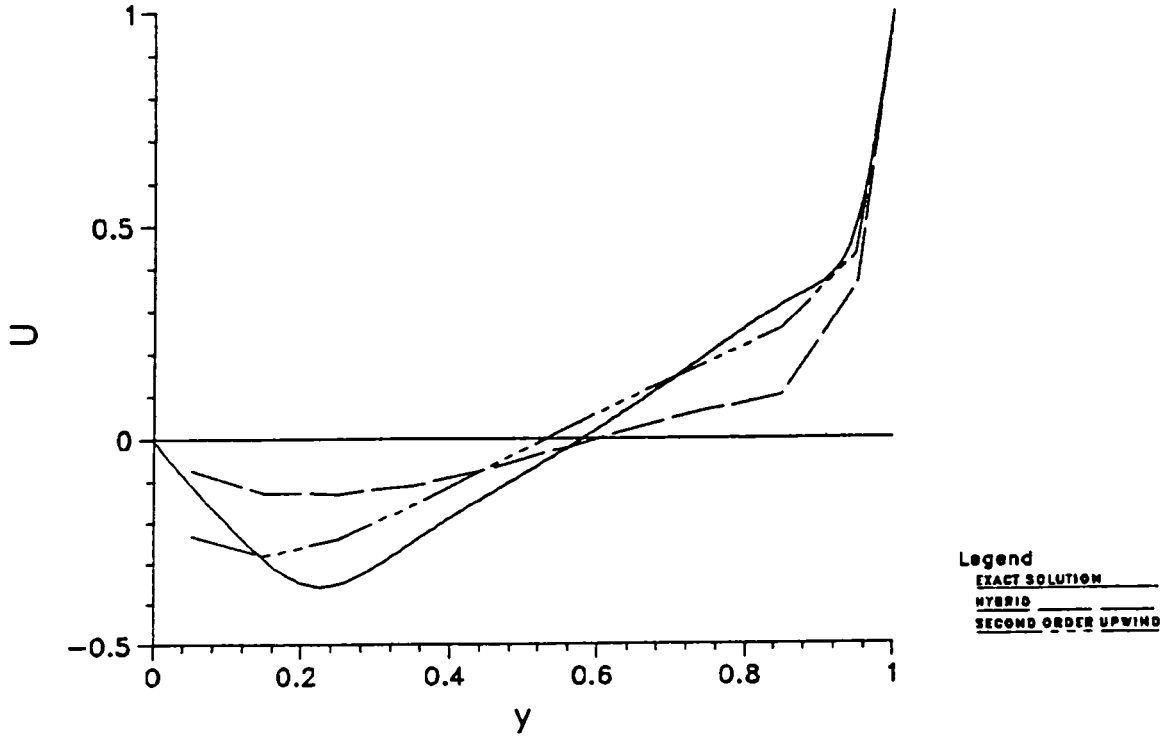

Fig. 21. Comparison of Vertical Center-line u-velocity Profile for Re = 600, 10x10 Grid

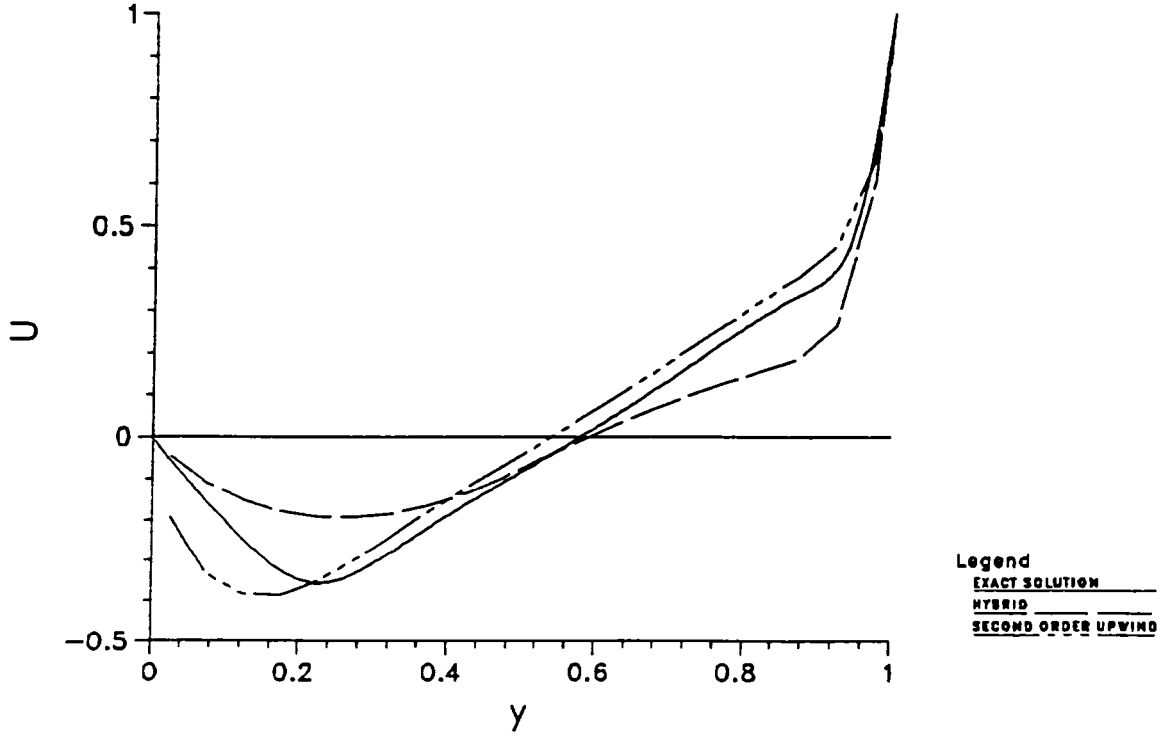

Fig. 22. Comparison of Vertical Center-line u-velocity Profile for Re = 600, 20x20 Grid

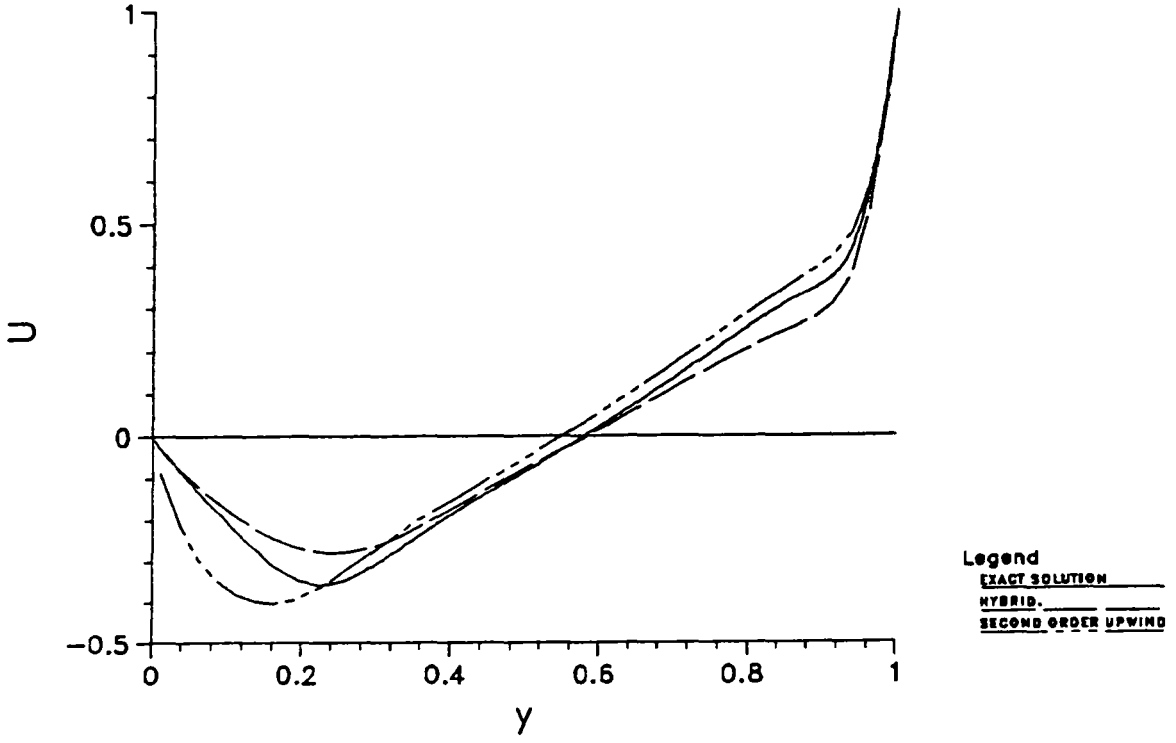

Fig. 23. Comparison of Vertical Center-line u-velocity Profile for Re = 600, 40x40 Grid

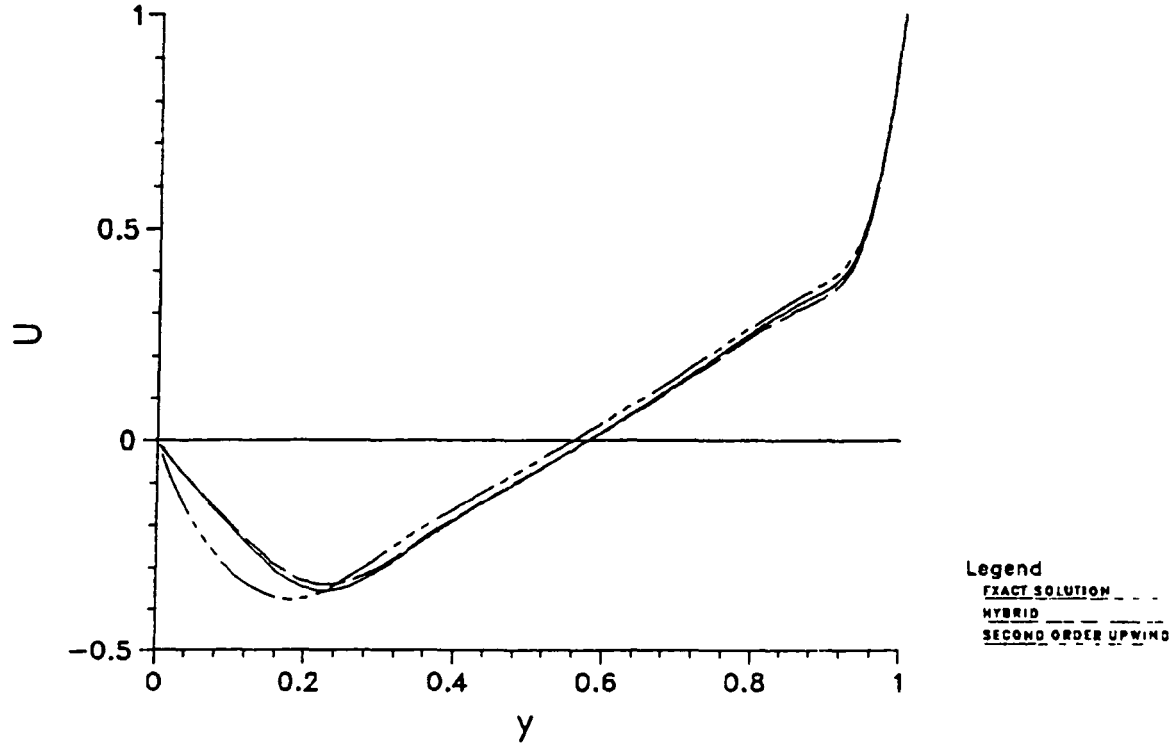

Fig. 24. Comparison of Vertical Center-line u-velocity Profile for Re = 600, 80x80 Grid

End of Document